Spherical Nucleic Acids as a Divergent Platform for Synthesizing RNA–Nanoparticle Conjugates through Enzymatic Ligation

Jessica L. Rouge,[†,‡] Liangliang Hao,[‡,§] Xiaochen A. Wu,[‡,§] William E. Briley,[‡,§] and Chad A. Mirkin[†,‡,*]

[†]Department of Chemistry and [‡]International Institute for Nanotechnology, [§]Interdisciplinary Biological Sciences Graduate Program, Northwestern University, 2145 Sheridan Road, Evanston, Illinois 60208-3113, United States

ABSTRACT Herein, we describe a rapid, divergent method for using spherical nucleic acids (SNAs) as a universal platform for attaching RNA to DNA-modified nanoparticles using enzyme-mediated techniques. This approach provides a sequence-specific method for the covalent attachment of one or more *in vitro* transcribed RNAs to a universal SNA scaffold, regardless of RNA sequence. The RNA–nanoparticle constructs are shown to effectively knock down two different gene targets using a single, dual-ligated nanoparticle construct.

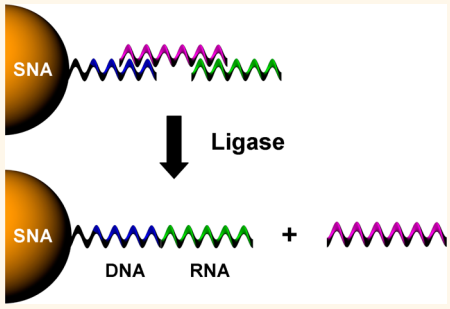

KEYWORDS: nanoparticle · enzymatic ligation · T4 DNA ligase · siRNA · gene knockdown

Nature has engineered rapid, highly sequence-specific enzymes capable of repairing spliced RNA and DNA molecules. These enzymes, known as ligases, catalyze the covalent attachment of the 3′ hydroxyl group of one oligonucleotide to the 5′ phosphate of another[1−3] with remarkable specificity. This specificity is made possible by the sequence information encoded in the terminal ends of oligonucleotide strands prior to their attachment to a given nucleic acid sequence. Indeed, ligation reactions have become powerful tools in various recombinant DNA-based technologies,[4−6] in genome sequencing,[7−9] and for synthesizing DNA–RNA heterostructures.[10−12]

Certain nucleic acid functionalized nanostructures have emerged as effective new tools for molecular diagnostics and intracellular gene regulation.[13−18] Specifically, nanoparticles conjugated to small interfering RNA (siRNA) have gained significant attention due to their ability to target mRNA for degradation in a sequence-specific manner. Despite their promising regulatory role in gene expression, siRNAs suffer from their inherent chemical instability in cellular environments. Many researchers have therefore developed methods for conjugating siRNA to the surface of nanoscale materials to improve the chance of successful delivery into cells. Chemical strategies including disulfide modification,[19] pegylation,[20] and the condensation of siRNA using polycations[21] have been used to facilitate the assembly of siRNAs on nanoparticles. Such constructs are typically synthesized by first functionalizing an oligonucleotide with an unnatural binding group (*e.g.*, alkylthiols or alkylamines) that can be adsorbed onto a particle of interest. This approach requires a specialty oligonucleotide to be synthesized for every nanoconstruct that one envisions. A potentially more appealing approach would be to prepare a universal construct that in a divergent manner can be used with readily accessible synthons to prepare a large set of constructs with the nucleic acids of interest.

In this regard, it would be extremely useful to be able to utilize ligases to interface relatively high cost RNA sequences

* Address correspondence to chadnano@northwestern.edu.

Received for review July 2, 2014 and accepted August 15, 2014.

Published online August 21, 2014
10.1021/nn503601s

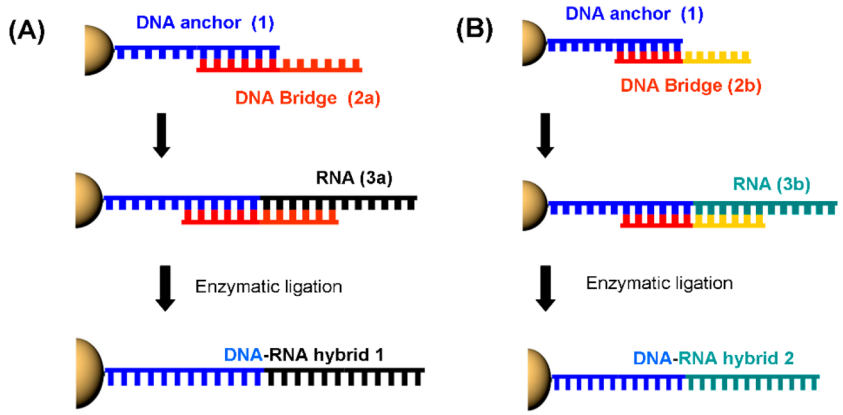

Figure 1. Enzyme-mediated assembly of RNA onto a universal SNA scaffold. (a) SNA consisting of a gold nanoparticle core modified with a DNA "anchor" oligonucleotide (1). A second DNA oligonucleotide, the DNA "bridge" (2a), is complementary to the 3′ end of 1. Upon hybridization with 1, the sticky end generated by the DNA bridge (2a) is used to guide the hybridization and assembly of the 5′ end of an RNA (3a) to the SNA surface. For siRNA sequences, this strand is the RNA sense strand of an siRNA duplex. (B) By changing the sequence of the sticky end of the DNA bridge at its 3′ end (2b), it can be made complementary to the 5′ end of a different RNA oligonucleotide (3b), thus allowing different RNA sequences to be assembled on an SNA passivated with the same DNA anchor (1).

with a readily available, low-cost DNA-nanoparticle construct. Herein, we describe a method for assembling siRNA on DNA-based spherical nucleic acid (SNA)[22] gold nanoparticle conjugates via a T4 DNA ligase-catalyzed reaction (Figure 1).

This is done in the context of a universal DNA-based SNA gold nanoparticle conjugate. SNAs often consist of a gold nanoparticle core that has been densely functionalized with DNA or siRNA oligonucleotides modified with terminal alkylthiols. SNAs have been shown to exhibit many desirable qualities as cellular transfection and gene regulation materials, including high cellular uptake and resistance to certain enzymatic degradation pathways.[18,23] Importantly, we find here that the sterically limiting SNA structure and its high local salt concentration, which can impede certain enzymatic systems,[23] does not prohibit enzymatic ligation. Moreover, the directionality of the DNA afforded by the SNA template allows one to attach RNA to specific ends of a nucleic acid sequence and avoids nonproductive cyclization reactions.

Enzyme-mediated assembly of siRNA on SNAs has two key advantages over the direct attachment of a chemically modified RNA to the surface of a nanoparticle. The first advantage is the practical reduction in cost and time it takes to assemble *in vitro* transcribed siRNA onto nanoparticles as opposed to synthesizing chemically modified RNA on an automated RNA synthesizer. Extensive purification and post processing of the modified RNA sequence over several days is required prior to use in assembly of an RNA–nanoparticle construct. In the case of *in vitro* RNA transcription, the reaction requirements are T7 RNA polymerase, a high-yielding RNA synthesizing enzyme,[24] a short double-stranded DNA (dsDNA) template, and millimolar solutions of ATP, GTP, CTP, UTP, and GMP. These individual nucleotide solutions in the presence of the dsDNA template and T7 RNA polymerase can generate high micromolar quantities of RNA in solution in under 2 h. In addition, the direct 5′ modification of the RNA with GMP during its enzymatic synthesis removes the need for post synthetic chemical modification of the RNA.

The second major advantage is programmability, as one can design the ligation reaction components to preassemble specific RNA sequences at an SNA surface based on the sequence information encoded in **2a**, the DNA bridge (Figure 1). The initial step of the ligation reaction involves two oligonucleotides (one DNA **1**, the other RNA **3a**) that are to be covalently attached through the generation of a new phosphodiester bond.[25] These oligonucleotides are assembled end-to-end (3′OH of DNA to 5′PO of RNA) through hybridization to **2a**. The DNA bridges therefore provide a powerful way to add one or more unique RNA sequences to the surface of an SNA in a single one-step enzymatic reaction. Once assembled, ligase can be added to the solution, resulting in the covalent attachment of the DNA anchor to the adjacent RNA oligonucleotide.

It is important to note that one key requirement for the ligation of RNA to DNA is that the RNA 5′ end must have a guanosine monophosphate (GMP) as opposed to the native triphosphate (GTP). This difference in phosphate units is a requirement for compatibility with the enzyme's mechanism of attachment[26,27] and the need for ATP when sealing the phosphodiester bond between the different oligonucleotide strands (Figure 1). Incorporation of a 5′ GMP modification is achieved via the *in vitro* transcription of RNA, wherein an excess of GMP relative to GTP (30:1) results in the end-labeling of the RNA transcript.[10] Once modified

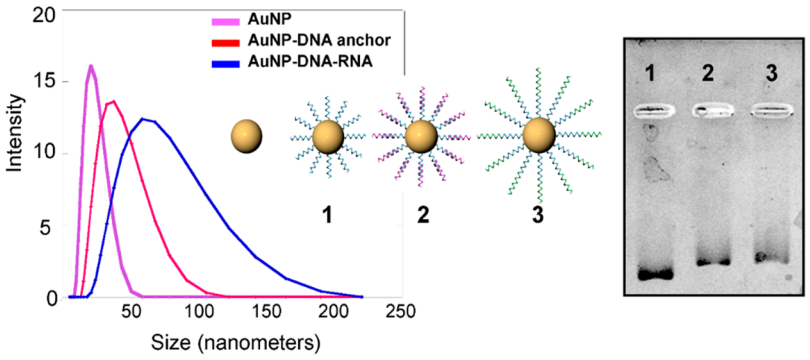

Figure 2. Size determination of ligated siRNA SNAs. (a) DLS data showing the increase in size between the citrate-capped 13 nm Au nanoparticles (pink), the SNAs modified with the DNA ligation anchor (red) and the final RNA-DNA chimera formed at the surface of the Au NPs (blue). (b) Electrophoretic mobility of the ligated siRNA SNA and its intermediates. DNA anchor functionalized SNA (lane one), DNA anchor modified SNA hybridized to the RNA specific DNA bridge (lane 2), fully ligated siRNA construct post treatment with T4 DNA ligase and removal of DNA bridge (lane 3).

with a terminal GMP residue, the RNA is purified and ligated to the SNA.

RESULTS AND DISCUSSION

In order to investigate the ligation efficiency of T4 DNA ligase for attaching RNA to a DNA-functionalized nanoparticle, SNAs were prepared using a 5′ hexyl dithiol DNA anchor (**1**) (Supporting Information, Table S1). Note that oligonucleotides may also be immobilized using readily available cyclic disulfides.[28] To accurately determine the average number of RNA strands ligated to the surface of the SNA, a new photocleavable assay was developed. In this assay, a second DNA anchor was synthesized in which a photocleavable (PC) linker was incorporated near the 3′ end of DNA anchor (Figure S1, Supporting Information). Upon irradiation with 365 nm light, the PC linker was cleaved, freeing the hybrid RNA−DNA oligonucleotides from the nanoparticle surface. The freed oligonucleotides were then isolated from the nanoparticles in solution via centrifugation and quantified using a fluorescence intercalation assay.[29] For 13 nm gold nanoparticles initially functionalized with 80 DNA anchor strands, there were 65 ± 5 RNA strands ligated per particle. Post ligation, the complementary antisense (AS) siRNA oligonucleotide was hybridized to the covalently attached sense strand (**3a**) in the presence of 1× PBS at 37 °C for 1 h. The total number of siRNA duplexes formed was 35 ± 5, illustrating that this approach can yield comparable coverages to that of conventional siRNA SNA architectures.[30,31]

We also assessed the increase in average particle size accompanying the enzymatic ligation reaction using dynamic light scattering (DLS) and agarose gel electrophoresis (Figure 2). After ligation, the particles were washed with 8 M urea and centrifuged to remove any excess DNA bridge that may remain after the ligation reaction was completed. DLS measurements showed the average size and polydispersity of the particles increased after ligation (Table S2, Supporting Information).

After characterization of the ligated siRNA SNAs, it was necessary to ensure that the biochemical recognition and therapeutic function of the siRNA was maintained after undergoing the enzymatic ligation strategy. To evaluate this, ligated RNA SNAs containing a siRNA sequence targeting green fluorescent protein (GFP) mRNA were fluorophore labeled with cyanine 5 (Cy5) to track the constructs intracellularly. Incubation of the Cy5-labeled siRNA−SNAs with a GFP-expressing cell line allows for simultaneous assays of uptake and biological function using flow cytometry. GFP fluorescence is then used as a proxy to infer relative GFP protein levels. The ligated GFP siRNA SNA constructs were readily taken up into mouse endothelial cells (Figure 3a−d) and able to reduce the expression of GFP protein by up to 53% relative to untreated cells (Figure 3e).

After establishing that the ligated siRNA SNAs maintain their biological activity, a second, dual siRNA construct consisting of two different siRNA sequences was assembled using the hybrid RNA−DNA ligation reaction. The ability to attach two different siRNA sequences to the same nanoparticle would enable a single construct to simultaneously target two different mRNAs in the same cell. An siRNA targeting GAPDH (a ubiquitous housekeeping gene)[32,33] was chosen as a second sequence to ligate alongside GFP siRNA on the SNA. The sense strand for each siRNA sequence was *in vitro* transcribed and ligated to the universal SNA scaffold. All sequences used in the construction of the dual siRNA SNAs are shown in Table S1 (Supporting Information). Each sense strand (**3a** and **3b**) was added to the ligation reaction in equal concentrations, allowing the 5′ end of the individual RNA sense strands (GFP or GAPDH siRNA) to assemble at the 3′ end of the SNA's DNA anchor (**1**) via hybridization with its respective DNA bridge (**2a** and **2b**) (Table S1, Supporting Information).

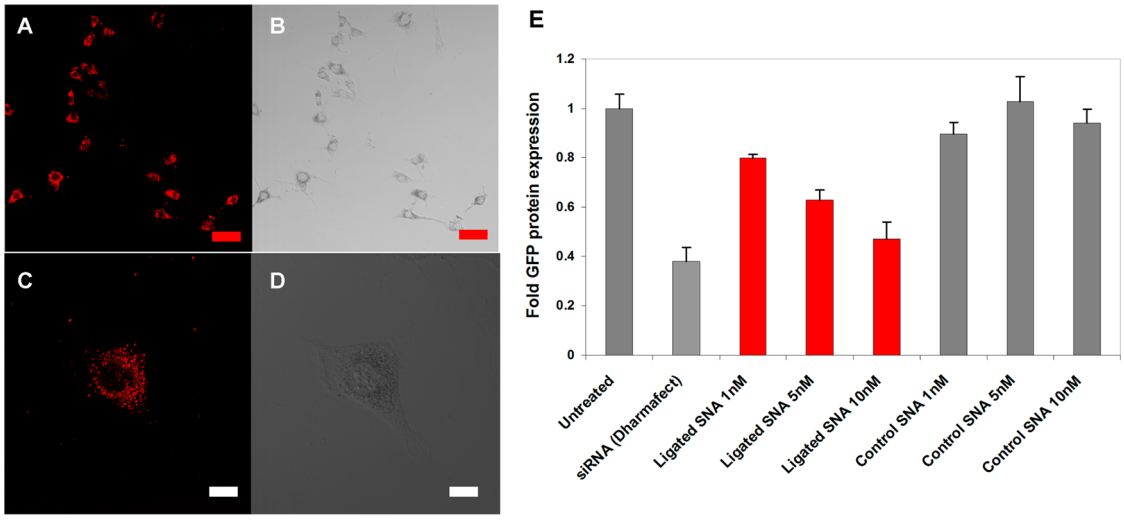

Figure 3. Cellular uptake and gene knockdown of GFP by siRNA ligated SNAs. (a) Confocal microscopy of C166 cells treated with 5 nM Cy5-labeled SNAs. (b) Same image as (a) without Cy5 filter. (c) Individual cell showing the diffuse uptake of the ligated SNAs into the cell as indicated by Cy5 fluorescence. (d) Corresponding bright field image of cell shown in (c). (e) Comparison of C166 GFP-expressing cells by flow cytometry showing relative changes in the amount of GFP protein expression post treatment with GFP siRNA ligated SNAs. Compared to the untreated cells, 10 nM treatment of the cells with the ligated SNAs resulted in 53% decrease in GFP expression. The ligated SNAs also follow a dose-dependent knockdown of GFP protein over the concentrations investigated. Scale bar is 50 μm in a, b and 10 μm in c, d.

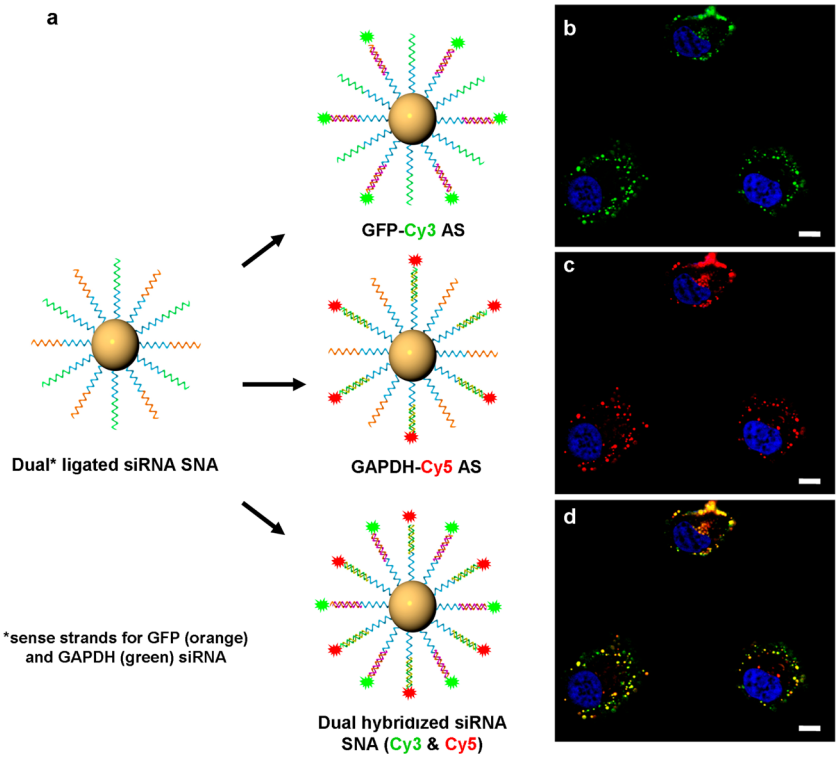

Figure 4. Assembly and localization of two siRNAs on a single SNA scaffold. (a) Schematic representation of the differential hybridization of fluorophore-labeled antisense RNA oligonucleotides on the same dually ligated SNA batch (particles ligated with both GFP 3a and GAPDH 3b siRNA). The SNA ligated to the GFP and GAPDH siRNA sense strands is then hybridized to either the GFP-Cy3 AS, GAPDH-Cy5 AS sequence, or both fluorophore-labeled AS sequences. (B) Dual hybridized SNAs viewed under Cy3 emission channel, pseudocolored as green. (c) Dual hybridized SNAs viewed under Cy5 emission channel. (d) Dual hybridized SNAs viewed under both Cy3 and Cy5 emission channels where colocalization of the fluorescence from the GFP and GAPDH AS strands is evident. Scale bar is 15 μm.

After ligation of the siRNA sense strands to the SNA scaffold, the constructs were incubated with both GFP and GAPDH antisense strands (**4a** and **4b**) to generate the final duplexed version of the particle. In order to track the ability of the AS siRNAs to hybridize to the same SNA as well as to visualize the constructs' post

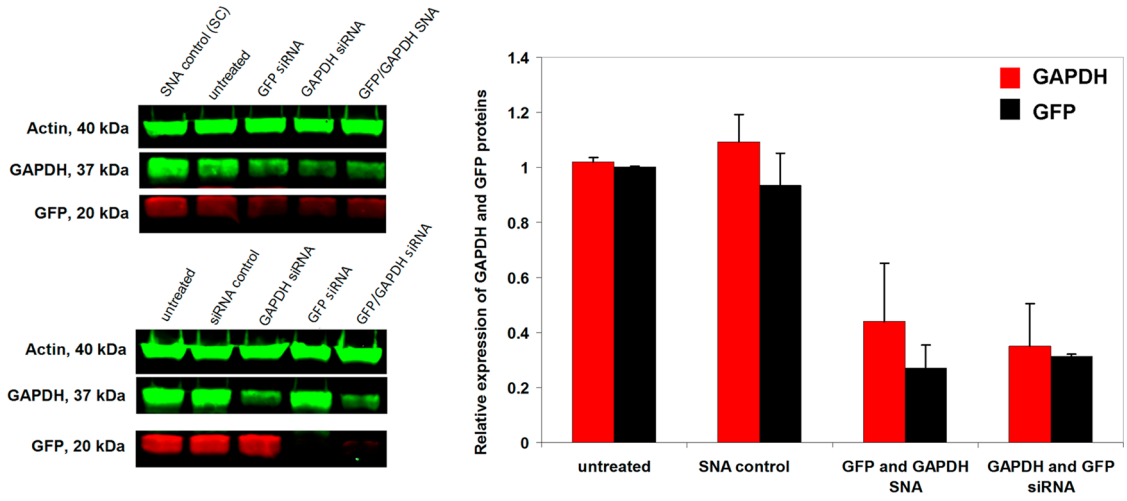

Figure 5. Targeted gene knockdown by dual-ligated siRNA SNAs. Compared with gene expression levels in untreated cells, both GFP and GAPDH protein expression levels are significantly reduced in GFP-C166 mouse cells treated with dual-ligated GFP/GAPDH SNAs. Error bars indicate standard deviation of the mean from three independent experiments. The same siRNA sequences transfected using the commercially available transfection agent, DharmaFect, served as a positive control.

cellular uptake, fluorophore-labeled versions of the GFP and GAPDH AS sequences (Cy3 and Cy5, respectively) were prepared and hybridized to the particles. The results of their uptake into HeLa cells are shown in Figure 4, in which fluorescence from both the GFP-Cy3 AS RNA and the GAPDH-Cy5 AS RNA are seen colocalized throughout the cells.

To investigate the sequence-specific RNAi capability of the dual siRNA SNA nanoparticle construct, the duplexed siRNA particles were incubated with C166 GFP-expressing cells (cells which also express the ubiquitous protein GAPDH) overnight. After treatment, the cells were lysed and the individual protein expression levels of GFP and GAPDH proteins were evaluated. Under this dual treatment, there was substantial knockdown of both GFP and GAPDH proteins as shown by Western blots, indicating both ligated siRNA sequences are biologically active (Figure 5). As shown by densitometry quantification of averaged triplicate Western blots (right panel, Figure 5), the effects of the dual siRNA SNA were comparable to those produced by traditional polymer-assisted siRNA transfections.

CONCLUSION

In summary, we have developed a robust and straightforward biochemical strategy for assembling RNA at the surface of an SNA while preserving its biological function. Using this method, two or more *in vitro* transcribed RNAs can be attached to an SNA through the use of programmable, sequence-specific DNA bridges. This enzyme-mediated approach opens up a rapid route for preparing single RNA–nanoparticle constructs capable of targeting multiple sites on a single mRNA transcript, as well as the ability to study the synergistic effects of targeting two different mRNA transcripts in related biochemical pathways. As the SNA assembly method has recently been expanded to include myriad nanoscale starting materials,[34] the assembly of RNA onto a variety of different materials can be realized quickly and efficiently, accelerating the study of RNA–NP-based delivery platforms for a wide array of biological applications.

MATERIALS AND METHODS

SNA Assembly and Characterization. Au NPs (13 nm) were functionalized with a 5′ hexyl dithiolated DNA anchor (Table S1, Supporting Information) purchased from Trilink Biotechnologies. The DNA anchor was first treated with DTT to activate the terminal thiol (C6 S–S phosphoramidite) and washed over Sephadex G-25 to remove any excess DTT. The DNA anchor is then incubated with 13 nm citrate-capped Au NPs and treated with 0.1% SDS buffered in 10 mM sodium phosphate buffer. Particles were salted to a final NaCl concentration of 0.3 M over the course of 5 h and washed 3× at 21130 rcf for 15 min to remove excess salts and DNA.

Quantification of RNA Loading onto SNA. The average number of DNA anchor molecules at the surface of each AuNP was determined by dissolving the AuNP with 40 mM KCN in 1× PBS. Once the gold is dissolved by KCN, the average number of DNA oligonucleotides per NP left in solution was determined using Sybr green, a DNA intercalator, and monitoring total emission at 520 nm on a fluorescence plate reader. To determine the average number of RNA strands ligated on the DNA anchor-functionalized SNAs, a photocleavable (PC) phosphoramidite was incorporated into a second DNA anchor molecule for analytical studies. The PC-modified DNA anchor (5′-SH-T30-PC-TTTTTAATTCACCCAAC-3′) was ordered from Trilink Biotechnologies and used as received without further purification. Using the same KCN method for dissolving the AuNPs, the PC DNA–SNAs were salted to 0.3 M NaCl and analyzed for total DNA anchor loading. Post ligation of GFP sense RNA (**3a**) and removal of excess bridge by washing 3× with 8 M urea and centrifuging at 21130 rcf for 6 min, the particles were irradiated

with 365 nm light for 10 min with mixing to initiate photocleavage. The particles were then centrifuged, and the supernatant was removed and analyzed using Sybr Green and a fluorescence plate reader to determine the total number of ligated siRNA strands. A 1% agarose gel showing the SNA mobility pre- and postirradiation with a PC DNA anchor is shown in Figure S1 (Supporting Information).

RNA *in Vitro* Transcription and Ligation. All RNA sense strands used in the ligation reactions and for assembly of siRNA SNAs were generated through *in vitro* transcription. The antisense strands later hybridized to the sense siRNA were synthesized using an automated RNA synthesizer (Mermaid) as no chemical modifications were needed for assembly on the nanoparticle surface. The dsDNA template for the transcription of the GFP sense RNA strand (**3a**) was transcribed using the ssDNA template 5′- GCTAATACGACTCACTATAGGGAG *GGCAAGCTGACCCTGAAG TTC*-3′ (sequence design based on a validated siRNA GFP sequence from Ambion). This ssDNA template was PCR amplified using the corresponding 3′ and 5′ primers, 5′-biotin-GAACTTCAGGGTCAGCTT-3′ and 5′-GCTAATACGACTCACTATAGGGAGAC-3′, respectively. The italicized half of the ssDNA template can be changed depending on the siRNA sequence of interest. All ssDNA templates and the forward and reverse primers were purchased from integrated DNA technologies (IDT). Through primer extension, the dsDNA was biotinylated by the 3′ primer, providing a facile route for immobilization on streptavidin-coated polystyrene beads and purification from the PCR reaction components. These dsDNA templated beads were then used for transcription with T7 RNA polymerase (Invitrogen). Transcription reactions were run for 2 h at 37 °C and contain the dsDNA template, T7 RNA polymerase, 1 mM ATP, CTP,GTP, UTP, DTT, and 30 mM GMP. After the reaction was complete, the solution was centrifuged, and the RNA remaining in the supernatant was removed and run through a size-exclusion column (Sephadex-25) to remove any excess nucleotides and residual DTT. Enzymatic ligation reactions containing the siRNA sense strand for GFP (**3a**), the corresponding DNA bridge molecule (**2a**), and DNA SNAs were then incubated at 37 °C overnight in a ratio of 1:2:5. The ligation reaction mixture included 5 mM ATP and 1× ligase buffer (Invitrogen) for maintaining enzyme stability. After ligation, the ligated siRNA SNAs were washed with 8 M urea 3× by centrifugation at 21130 rcf for 12 min intervals. This is to ensure removal of the enzyme and any residual nucleic acids that were not ligated to the surface of the SNA. The same procedure was performed for the GAPDH sequence (**3b**) using bridge **2b** (Table S1, Supporting Information). To generate the duplexed siRNA structure at the SNA surface, the corresponding antisense siRNA sequences were hybridized to the ligated siRNA SNAs by incubation with 10 μM solutions of the respective AS siRNA sequences (**4a** and **4b** for GFP and GAPDH respectively) at 37 °C in 1× PBS for 1 h, followed by centrifugation at 21130 rcf 3× to remove excess AS siRNA that did not hybridize to the SNA. The same procedure was followed to prepare the fluorophore-labeled versions of the siRNA SNAs for cellular uptake studies.

Dynamic Light Scattering (DLS). SNAs pre- and postligation were analyzed using a Malvern Zetasizer instrument. SNA samples were washed 3× in H_2O and centrifuged at 21130 rcf prior to DLS measurements. All samples were run in triplicate with five scans averaged per sample analyzed.

Agarose Gel Electrophoresis. Ligated RNA-SNAs were analyzed using 1% agarose gels run at 90 V for 30 min in 0.5× TAE buffer. Gels were imaged on a Fujifilm gel imager using 1× Sybr gold stain.

Confocal Microscopy and Cellular Uptake Studies. For the single siRNA sequence SNA, cell uptake studies were evaluated through the use of a Cy5-DNA probe backfilled onto the SNA surface during the initial AuNP functionalization step. The Cy5-DNA probe was incorporated on to the ligated GFP siRNA−SNA nanoparticles by initially functionalizing the AuNPs with a 5:1 ratio of 5′-thiolated DNA anchor (**1**) to a 5′-thiolated polyT$_{20}$-Cy5 DNA oligonucleotide. These particles were then ligated with the GFP siRNA sense strand (**3a**) through the methods described above. The particles were added to the media of C166 GFP-expressing cells. All cells were cultured at 37 °C and 5% CO_2 in DMEM supplemented with 10% FBS and 1% streptomycin/penicillin unless specified otherwise. Seeded sparsely in a 35 mm FluoroDish (World Precision Instruments), C166-GFP cells were grown overnight before being incubated with 5 nM of Cy5-labeled siRNA-SNAs in OptiMEM for 8 h. Cells were then rinsed with PBS, fixed in 3.7% PFA in PBS for 15 min, and imaged under a Zeiss LSM 510 inverted confocal microscope. The excitation wavelength of Cy5 was 633 nm, and the corresponding emission filter was 660−710 nm.

The dual-ligated GFP/GAPDH siRNA SNAs were analyzed by confocal microscopy through fluorophore labeling of the AS siRNA strands (**4a** and **4b**) with Cy3 and Cy5. Their uptake was evaluated in HeLa cells using a Lecia SP5 multilaser confocal microscope. The Lecia confocal microscope was used for observing multiple fluorescent probes (Cy3 and Cy5 channels) and tracking the colocalization of fluorescence within the cells. HeLa cells were treated with 1 nM dually ligated SNAs for 24 h in OptiMEM, followed by one wash with PBS, and resuspension in DMEM.

Flow Cytometry Studies. Total GFP protein level was analyzed using a Guava benchtop flow cytometer, using fluorescence intensity to proxy for protein level. Cells were seeded at 25% confluency in 96-well plate format 24 h prior to SNA treatment. Ligated siRNA SNAs and control constructs were incubated with these cells in OptiMEM for 16 h before media exchange into fresh, complete DMEM for an additional 48 h of recovery time. After treatment, cells were thoroughly washed with PBS and detached using trypsin before directly assayed live by flow cytometry (Guava 8HT, Millipore).

Western Blot Analysis. C166 cells were plated in a 6-well cell culture dish and incubated with 1 mL of particles (5 nM of nanoparticles in OptiMEM medium) or transfected with 200 nM of siRNAs using commercially available DharmaFect reagent overnight. Cells were washed three times with PBS and homogenized in 0.1 mL of ice-chilled mammalian cell lysis buffer containing 1× protease and phosphatase inhibitor (Thermo Scientific). The homogenate were cleared by centrifugation at 18406 rcf for 5 min, and the supernatant was kept as protein lysis. Total protein amount in the lysis was quantified using Pierce BCA Protein Assay Kit. The lysis with same amount of total protein was transferred to a 1.5 mL microcentrifuge tube and incubated with an equal volume of dithiothreitol (DTT)-containing loading buffer (54 mg/mL). After being boiled for 5 min, samples with equal amounts of total proteins were fractionated by 4−20% precast gradient gel (Bio-Rad). The intact gel was then transferred to nitrocellulose membranes (Thermo Scientific) and blocked in odyssey blocking buffer (LI-COR Biosciences). Proteins were detected with primary antibodies against GAPDH (1:500) (Santa Cruz Biotechnology), GFP (1:1000) (Clontech Laboratories Inc.), and β-actin (1:1000) (Cell Signaling Technology), followed by IRDye 680/800 secondary antibodies (1:10000−1:5000) (LI-COR Biosciences) diluted in PBST containing 5% nonfat milk. The desired bands were visualized using the Odyssey CLx Infrared Imaging System (LI-COR Biosciences).

Conflict of Interest: The authors declare no competing financial interest.

Supporting Information Available: RNA and DNA sequence information, photocleavable gel shift assay, and tabulated DLS measurements. This material is available free of charge via the Internet at http://pubs.acs.org

Acknowledgment. This work was supported by the Defense Advanced Research Projects Agency HR0011-13-2-0018 and the Center for Cancer Nanotechnology Excellence (CCNE) initiative of the National Institutes of Health (NIH) U54 CA151880. J.L.R. acknowledges a postdoctoral fellowship from the PhRMA foundation. L.H. is a Howard Hughes Medical Institute International Student Research Fellow and acknowledges a Ryan Fellowship from Northwestern University. Confocal imaging was performed at the Biological Imaging Facility (BIF) at Northwestern University.

REFERENCES AND NOTES

1. Timson, D. J.; Singleton, M. R.; Wigley, D. B. DNA Ligases in the Repair and Replication of DNA. *Mutat. Res.* **2000**, *460*, 301–318.

2. Weiss, B.; Thompson, A.; Richardson, C. C. Enzymatic Breakage and Joining of Deoxyribonucleic Acid. *J. Biol. Chem.* **1968**, *243*, 4556–4563.
3. Lehman, I. R. DNA Ligase: Structure, Mechanism, and Function. *Science* **1974**, *186*, 790–797.
4. Nuttle, X.; Itsara, A.; Shendure, J.; Eichler, E. E. Resolving Genomic Disorder—Associated Breakpoints within Segmental DNA Duplications Using Massively Parallel Sequencing. *Nat. Protoc.* **2014**, *9*, 1496–1513.
5. Li, Y.; Wark, A. W.; Lee, H. J.; Corn, R. M. Single-Nucleotide Polymorphism Genotyping by Nanoparticle-Enhanced Surface Plasmon Resonance Imaging Measurements of Surface Ligation Reactions. *Anal. Chem.* **2006**, *78*, 3158–3164.
6. Wark, A. W.; Lee, H. J.; Qavi, A. J.; Corn, R. M. Nanoparticle-Enhanced Diffraction Gratings for Ultrasensitive Surface Plasmon Biosensing. *Anal. Chem.* **2007**, *79*, 6697–6701.
7. Drmanac, R.; Sparks, A. B.; Callow, M. J.; Halpern, A. L.; Burns, A. L.; Kermani, B. G.; Carnevali, P.; Nazarenko, I.; Nilsen, G. B.; Yeung, G.; *et al.* Human Genome Sequencing Using Unchained Base Reads on Self-Assembling DNA Nanoarrays. *Science* **2010**, *327*, 78–81.
8. Yegnasubramanian, S. Preparation of Fragment Libraries for Next-Generation Sequencing on the Applied Biosystems SOLiD Platform. *Methods Enzymol.* **2013**, *529*, 185–200.
9. Shendure, J.; Hanlee, J. Next-Generation DNA sequencing. *Nat. Biotechnol.* **2008**, *26*, 1135–1145.
10. Holley, B. L.; Eaton, B. E. Methods for Selecting Catalytic Nucleic Acids. In *Evolutionary Methods in Biotechnology*; Brakmann, S, Schwienhorst, A., Eds.; John Wiley and Sons: Weinheim, 2004; pp 99—103.
11. Zhou, W.-J.; Chen, Y.; Corn, R. M. Ultrasensitive Microarray Detection of Short RNA Sequences with Enzymatically Modified Nanoparticles and Surface Plasmon Resonance Imaging Measurements. *Anal. Chem.* **2011**, *83*, 3897–3902.
12. Tarasow, T. M.; Tarasow, S. L.; Eaton, B. E. RNA-catalysed Carbon—Carbon Bond Formation. *Nature* **1997**, *389*, 54–57.
13. Prigodich, A. E.; Seferos, D. S.; Massich, M. D.; Giljohann, D. A.; Lane, B. C.; Mirkin, C. A. Nano-Flares for mRNA Regulation and Detection. *ACS Nano* **2009**, *3*, 2147–2152.
14. Zheng, D.; Seferos, D. S.; Giljohann, D. A.; Patel, P. C.; Mirkin, C. A. Aptamer Nano-Flares for Molecular Detection in Living Cells. *Nano Lett.* **2009**, *9*, 3258–3261.
15. Rosi, N. L.; Mirkin, C. A. Nanostructures in Biodiagnostics. *Chem. Rev.* **2005**, *105*, 1547–1562.
16. Storhoff, J. J.; Lucas, A. D.; Garimella, V.; Bao, Y. P.; Müller, U. R. Homogeneous Detection of Unamplified Genomic DNA Sequences Based on Colorimetric Scatter of Gold Nanoparticle Probes. *Nat. Biotechnol.* **2004**, *22*, 883–887.
17. Agasti, S. S.; Rana, S.; Park, M.-H.; Kim, C. K.; You, C.-C.; Rotello, V. M. Nanoparticles for Detection and Diagnosis. *Adv. Drug Delivery Rev.* **2010**, *62*, 316–328.
18. Rosi, N. L.; Giljohann, D. A.; Thaxton, C. S.; Lytton-Jean, A. K. R.; Han, M. S.; Mirkin, C. A. Oligonucleotide-Modified Gold Nanoparticles for Intracellular Gene Regulation. *Science* **2006**, *312*, 1027–1030.
19. Lee, J. S.; Green, J. J.; Love, K. T.; Sunshine, J.; Langer, R.; Anderson, D. G. Gold, Poly(β-amino ester) Nanoparticles for Small Interfering RNA Delivery. *Nano Lett.* **2009**, *9*, 2402–2406.
20. Liu, Z.; Winters, M.; Holodniy, M.; Dai, H. siRNA Delivery into Human T Cells and Primary Cells with Carbon-Nanotube Transporters. *Angew. Chem., Int. Ed.* **2007**, *46*, 2023–2027.
21. Jeong, J. H.; Mok, H.; Oh, Y.-K.; Park, T. G. siRNA Conjugate Delivery Systems. *Bioconjugate Chem.* **2009**, *20*, 5–14.
22. Cutler, J. I.; Auyeung, E.; Mirkin, C. A. Spherical Nucleic Acids. *J. Am. Chem. Soc.* **2012**, *134*, 1376–1391.
23. Seferos, D. S.; Prigodich, A. E.; Giljohann, D. A.; Patel, P. C.; Mirkin, C. A. Polyvalent DNA Nanoparticle Conjugates Stabilize Nucleic Acids. *Nano Lett.* **2008**, *9*, 308–311.
24. Wyatt, J. R.; Chastain, M.; Puglisi, J. D. Synthesis and Purification of Large Amounts of RNA Oligonucleotides. *BioTechniques* **1991**, *11*, 764–769.
25. Ellenberger, T.; Tomkinson, A. E. Eukaryotic DNA Ligases: Structural and Functional Insights. *Annu. Rev. Biochem.* **2008**, *77*, 313–338.
26. Silverman, S. K. Practical and general synthesis of 5′-adenylated RNA (5′-AppRNA). *RNA* **2004**, *10*, 731–746.
27. Gumport, R. I.; Lehman, I. R. Structure of the DNA Ligase-Adenylate Intermediate: Lysine (ε-amino)-Linked Adenosine Monophosphoramidate. *Proc. Natl. Acad. Sci. U.S.A.* **1971**, *68*, 2559–2563.
28. Letsinger, R. L.; Elghanian, R.; Viswanadham, G.; Mirkin, C. A. Use of a Steroid Cyclic Disulfide Anchor in Constructing Gold Nanoparticle-Oligonucleotide Conjugates. *Bioconjugate Chem.* **2000**, *11*, 289–291.
29. Zipper, H.; Brunner, H.; Bernhagen, J.; Vitzthum, F. Investigations on DNA Intercalation and Surface Binding by SYBR Green I, its Structure Determination and Methodological Implications. *Nucleic Acids Res.* **2004**, *32*, 103–113.
30. Giljohann, D. A.; Seferos, D. S.; Prigodich, A. E.; Patel, P. C.; Mirkin, C. A. Gene Regulation with Polyvalent siRNA-nanoparticle Conjugates. *J. Am. Chem. Soc.* **2009**, *131*, 2072–2073.
31. Patel, P. C.; Hao, L.; Yeung, W. S. A.; Mirkin, C. A. Duplex End Breathing Determines Serum Stability and Intracellular Potency of siRNA-Au NPs. *Mol. Pharmaceutics* **2011**, *8*, 1285–1291.
32. Barber, R. D.; Harmer, D. W.; Coleman, R. A.; Clark, B. J. GAPDH as a Housekeeping Gene: Analysis of GAPDH mRNA Expression in a Panel of 72 Human Tissues. *Physiol. Genomics* **2005**, *21*, 389–395.
33. Alvarez-Erviti, L.; Seow, Y.; Yin, H.; Betts, C.; Lakhal, S.; Wood, M. J. A. Delivery of siRNA to the Mouse Brain by Systemic Injection of Targeted Exosomes. *Nat. Biotechnol.* **2011**, *29*, 341–345.
34. Zhang, C.; Macfarlane, R. J.; Young, K. L.; Choi, C. H. J.; Hao, L.; Auyeung, E.; Liu, G.; Zhou, X. Z.; Mirkin, C. A. A General Approach to DNA-programmable Atom Equivalents. *Nat. Mater.* **2013**, *12*, 741–746.